Chemical Papers (2022) 76:4309–4321
https://doi.org/10.1007/s11696-022-02178-0

ORIGINAL PAPER

Eco-friendly synthesis and characterizations of Ag/AgO/Ag_2O nanoparticles using leaf extracts of *Solanum elaeagnifolium* for antioxidant, anticancer, and DNA cleavage activities

Mukul Barwant[1] · Yogrsh Ugale[1] · Suresh Ghotekar[2] · Parita Basnet[3] · Van-Huy Nguyen[4] · Shreyas Pansambal[5] · H. C. Ananda Murthy[6] · Mika Sillanpaa[7,8] · Muhammad Bilal[9] · Rajeshwari Oza[10] · Vanita Karande[11]

Received: 22 November 2021 / Accepted: 14 March 2022 / Published online: 30 March 2022

Abstract

The biogenic synthesis of nanoparticles (NPs) using a plant extract is rapid, simple, efficient, cost-effective, and eco-friendly. This study investigated selective pharmacological activities such as anticancer, antioxidant, and DNA cleavage of *S. elaeagnifolium*-mediated green synthesizing Ag/AgO/Ag_2O NPs. To the best of our knowledge, *S. elaeagnifolium* has been the first time used to synthesize Ag/AgO/Ag_2O NPs. The synthesized NPs were explored by using UV–Vis diffuse reflectance spectroscopy, X-ray diffraction, Fourier transform infrared spectroscopy, scanning electron microscopy, high-resolution transmission electron microscopy, energy-dispersive X-ray spectroscopy, and photoluminescence analyses. Anticancer activity of Ag/AgO/Ag_2O NPs was tested on lung cancer cell lines (A-549) and showed activity at the IC_{50} of 67.09 µg/mL. The maximum 2,2′-azino-bis-3-ethylbenzthiazoline-6-sulphonic acid (ABTS) and 2,2-diphenyl-1-picrylhydrazyl (DPPH) scavenging activity were 25.78% and 20.86% at 100 µg/L, respectively. Moreover, *S. elaeagnifolium*-mediated green synthesized Ag/AgO/Ag_2O NPs exhibited considerable DNA cleavage activity. These results assured that the synthesized Ag/AgO/Ag_2O NPs using *S. elaeagnifolium* leaves extract may have potential applications in biomedical engineering.

Graphical abstract

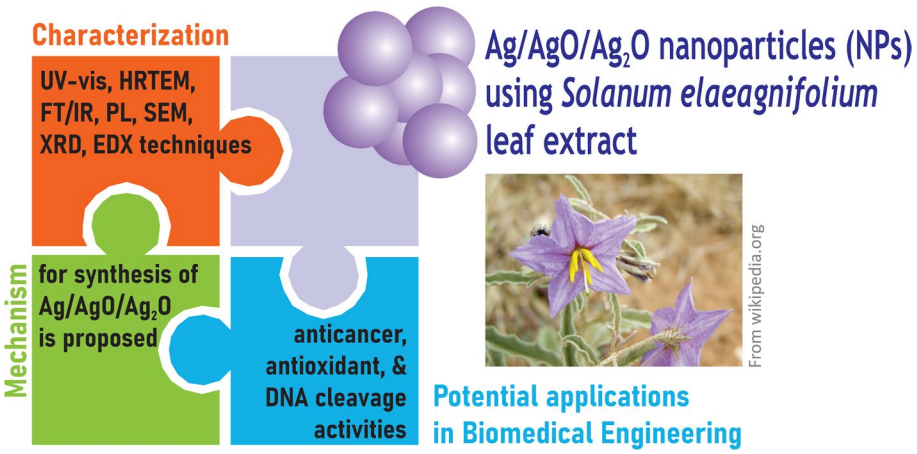

Keywords Green nanotechnology · *Solanum elaeagnifolium* · Ag/AgO/Ag_2O NPs · Biomedical applications

✉ Suresh Ghotekar
ghotekarsuresh7@gmail.com

Extended author information available on the last page of the article

Abbreviations

Ag	Silver
DFT	Density functional theory
DMSO	Dimethyl sulphoxide
DNA	Deoxyribonucleic acid

EDTA	Ethylenediamine tetraacetic acid
EDX	Energy-dispersive X-ray spectroscopy
FTLR	Fourier transform infrared spectroscopy
HRTEM	High-resolution transmission electron microscopy
IC_{50}	Half maximal inhibitory concentration
MTT	3-(4,5-Dimethylthiazol-2-Yl)-2,5-Diphenyltetrazolium Bromide
NPs	Nanoparticles
PL	Photoluminescence
SAED	Selected area electron diffraction
SELE	*Solanum elaeagnifolium* Leaves extract
SEM	Scanning electron microscopy
UVDRS	UV–Vis diffuse reflectance spectroscopy
XRD	X-ray diffraction

Introduction

Nowadays, nanotechnology has stupendous and enormous applications in many sectors of applied science and engineering like agriculture, biotechnology, dye degradation, food technology, wastewater treatment, energy, storage, ceramics, cosmetics, medical applications, drug delivery, bio-sensing, fabric, and textile engineering, etc. (Lin 2015; Thanh et al. 2014; Devadas et al. 2021; Gawande et al. 2016). In particular, metal oxide nanoparticles (NPs) have attracted extensive attention.

Many types of NPs, such as Ag_2O (Ghotekar et al. 2020), SnO_2 (Matussin et al. 2020), CdO (Ghotekar 2019), CuO (Cuong et al. 2021), Fe_3O_4 (Yew et al. 2020), ZnO (Bandeira et al. 2020), and ZrO_2 (Nikam et al. 2019), have been prepared and applied in various promising applications. They could be manufactured by biological, chemical, and physical approaches; nevertheless, biological protocols are the most recommended and sustainable approach since chemical, and physical approaches have numerous downsides (Gawande et al. 2016). Notably, the eco-friendly approach makes use of algae (AlNadhari et al. 2021), bio-waste materials (Santhosh et al. 2021; Dabhane et al. 2021), microorganisms (Ibrahim et al. 2021), and plants (Cuong et al. 2021). Green synthesis using various medicinal plant parts is most rapid, simple, clean, easy, affordable, and environmentally gracious (Soni et al. 2021). The varied plant parts contain a variety of structurally diverse natural biochemicals such as vitamins, alkaloids, anthocyanins, flavonoids, coumarins, phenols, sugars, glycosides, volatile oils, saponins, tannins, which themselves serve as bio-reducing and/or bio-stabilizing agents for NPs production and hence obviating the use of noxious chemicals and solvents (Nasrollahzadeh et al. 2020).

Among diverse NPs, silver-based NPs, such as Ag, AgCl, Ag_2O, and Ag_2S NPs, are creating spectacular attention in the scientific arena due to their massive range of application in agriculture (Partila 2019), biomedical devices (Singh et al. 2017), catalysis (Bhosale and Bhanage 2015), ceramics (Göl et al. 2020), environmental remediation (Ghotekar et al. 2020, 2021), pharmaceuticals (Durán et al. 2016), photocatalysis (Ghotekar et al. 2020, 2021; Marimuthu et al. 2020), and sensing (Tagad et al. 2013). The selective morphology and size of the silver-based NPs determine their chemical and physical features (Sharma et al. 2021). Heretofore, various approaches, such as the hydrothermal method (Yang and Pan 2012), microwave-assisted method (Al-Shehri et al. 2020; Babu et al. 2018), sol–gel method (Shahjahan et al. 2017), thermal decomposition (Hosseinpour-Mashkani and Ramezani 2014), have been reported for the manufacturing of silver-based NPs. However, these strategies are highlighted by high manufacturing costs and hazardous substances, which have possibly harmful impacts on human health and the environment. The green synthesis approach, based primarily on plant extracts, is an environmentally benign alternative to handling harmful chemicals in the manufacture of NPs. Noxious chemicals are replaced in these regimens by compounds derived from plant extracts that act as reductants and stabilizers (Aygün et al. 2020; Gur et al. 2022). Previously, facile biosynthesis of silver-based NPs using plant extracts such as *Acanthospermum hispidum* (Ghotekar et al. 2019), *Centella Asiatica* (Rashmi et al. 2020), *Prunus persica* (Patra and Baek 2016), and *Cochlospermum Gossypium* (Ayodhya and Veerabhadram 2016) have been reported as a bio-reducing/bio-stabilizing agent, and their multifunctional applications are widely investigated.

Noticeably, *Solanum elaeagnifolium* of the family *Solanaceae* is a deep-rooted perennial plant that is found initially native to the Americas. As summarized in Fig. 1, *Solanum elaeagnifolium* extract contains several bioactive compounds, namely stigmasterol, kaempferol, C-glycoside, quercetin, mangiferin, rutin, chlorogenic acid, coumaroyl glycoside, dicaffeoyl quinic acid (Badawy et al. 2013; Elabbar et al. 2014; Balah and AbdelRazek 2020). Also, leaves from *Solanum elaeagnifolium* have repellent and insecticidal characteristics towards various crop pests and possibly be used as an alternative for synthetic insecticides (Hamouda et al. 2015). However, to the best of our knowledge, *Solanum elaeagnifolium* has been examined for its pharmacological effects, but it has never been employed to synthesize Ag/AgO/Ag_2O NPs.

Herein, this contribution reports on Ag/AgO/Ag_2O NPs engineered by an entirely green chemistry approach using *Solanum elaeagnifolium* natural extract as a fuel addition of any chemical additives. The synthesized Ag/AgO/Ag_2O NPs were explored by various techniques to characterize the material further. In addition, selective biomedical applications such as anticancer, antioxidant, and DNA cleavage activities were also investigated.

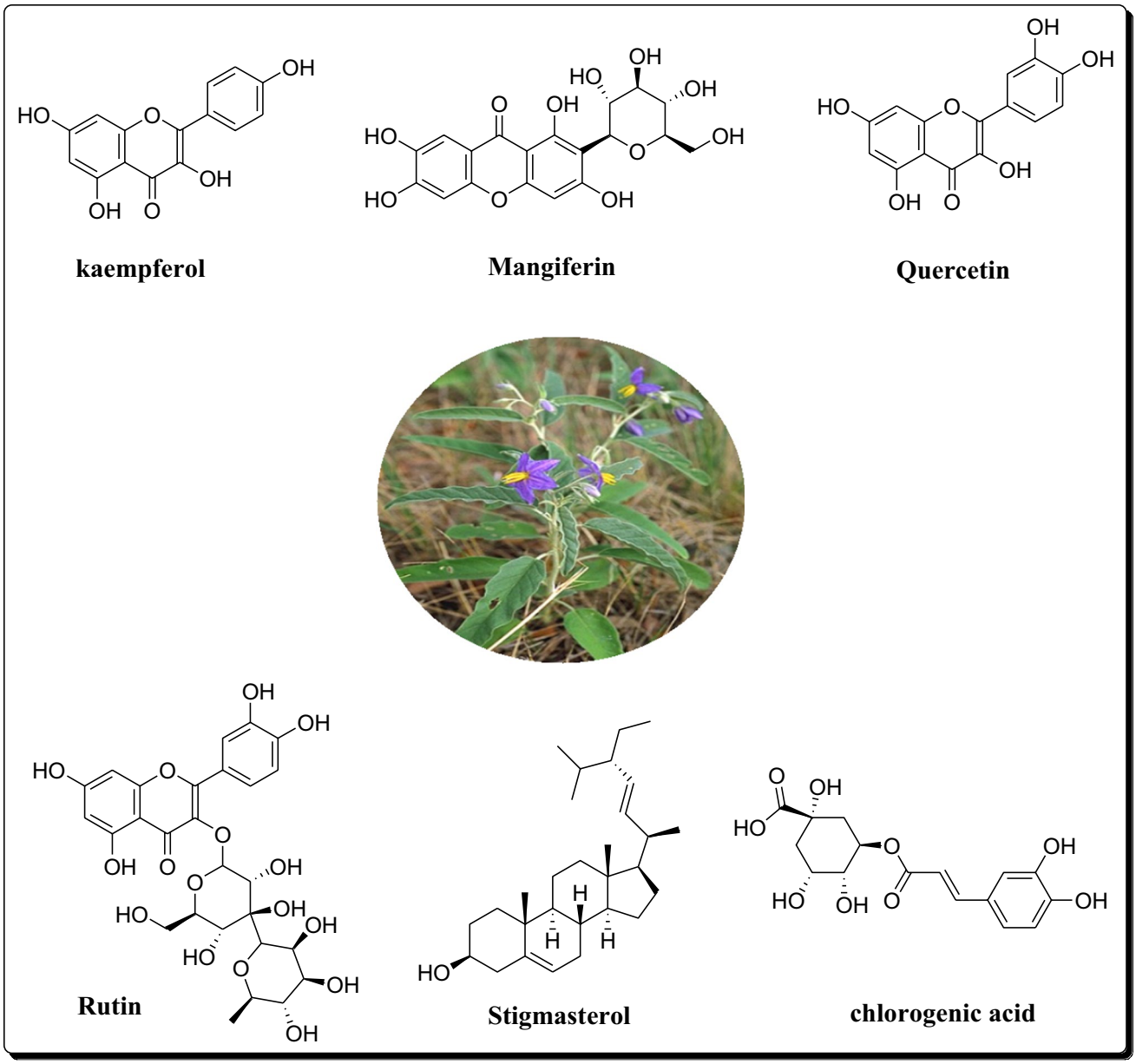

Fig. 1 Active phytochemicals in *Solanum elaeagnifolium*

Experimental

Collection of *Solanum elaeagnifolium* leaves and extracts preparation

The *Solanum elaeagnifolium* leaves were collected and appropriately washed using double distilled water. First, 5 g of leaves were poured into 100 mL of distilled water and boiled for 15 min at 85–90 °C. Next, the extract obtained was filtered through ordinary filter paper and Whatman No. 1 filter paper. Finally, the filtered *Solanum elaeagnifolium* leaves extract (SELE) was stored at 4 °C for the synthesis of Ag/AgO/Ag_2O NPs.

Biosynthesis of Ag/AgO/Ag_2O NPs

Eco-benign synthesis of Ag/AgO/Ag_2O NPs involved adding 1.69 g silver nitrate to 100 mL of SELE, and then the reaction solution was continuously stirred at 1100 rpm for 30 min at room temperature with a magnetic stirrer. Initial confirmation of Ag/AgO/Ag_2O NPs synthesis is by a change in color of the reaction mixture from yellow to dark brown. Then, the resulting solution was then centrifuged at room

temperature for 10 min at 3000 rpm and carefully washed to eliminate all the unwanted impurities. After removing the unwanted supernatant liquid, the black precipitate of material was placed in a hot air oven at 200 °C. The as-synthesized Ag/AgO/Ag_2O NPs were then crushed into a powder using mortar and pestle. The obtained black color powder was stored in an airtight vial for further utilization.

Characterization of Ag/AgO/Ag_2O NPs

Various characterization tools were used to examine the chemical, optical, and physical properties of Ag/AgO/Ag_2O NPs. The XRD measurement of synthesized Ag/AgO/Ag_2O NPs was carried out using a diffractometer system (XPERT-PRO, PANalytical). The UVDRS of Ag/AgO/Ag_2O NPs were recorded using Jasco Spectrophotometer V-770. The functional group's analysis of biosynthesized Ag/AgO/Ag_2O NPs was studied using FT-IR-4600 typeA. The morphological features and elemental composition of bio-fabricated Ag/AgO/Ag_2O NPs were analyzed by SEM equipped with an EDX detector (VEGA3 TESCAN). Moreover, size and shape were studied using HRTEM (JEM-2100) operating at an accelerating 60–200 kV voltage. The photoluminescence nature of SELE-mediated Ag/AgO/Ag_2O NPs was examined using FP-8200 Spectroflurimeter.

Anticancer activity of Ag/AgO/Ag_2O NPs

A549 lung cancer cells were procured from ATCC (American Type Culture Collection). Procured stock cells were grown in DMEM/RPMI supplemented with 10% inactivated Fetal Bovine Serum (FBS), penicillin (100 IU/ml), and streptomycin (100 µg/ml) in a humid environment of 5% CO_2 at 37 ºC. The cell was dissociated with cell dissociating solution (0.02% EDTA, 0.2% trypsin, and 0.05% glucose in PBS). The vitality of the cells is tested, and the cells are centrifuged. In addition, 50,000 cells/well were seeded in a 96 well plate and incubated at 37 ºC under a 5% CO_2 incubator for 24 h. Different concentrations of Ag/AgO/Ag_2O NPs (10, 20, 40, 80, 160, and 320 µg/mL) was added and incubated at 37 ºC for 48 h (Gonzalez and Tarloff 2001). The resulting solutions in the wells were removed after incubation, and 100 µl of MTT (5 mg/10 ml of MTT in PBS) was mixed with every well. The cultured plates were incubated at 37 °C for 4 h under a 5% CO_2 environment. The supernatant was discarded, and 100 µl of DMSO was mixed into the plates, which were gently agitated to dissolve the formed formazan (Sangeethaa et al. 2021). An ELISA reader measured the viability of cell lines was measured at 570 nm by an ELISA reader. Triplicates of experiments were carried out, and Doxorubicin standard drug was used in the study as a positive control. The cell viability percentage was estimated by using the formula,

$$\% \text{ Cell Inhibition} = \frac{A_{570} \text{ of test}}{A_{570} \text{ of control}} \times 100$$

In vitro antioxidant activity of Ag/AgO/Ag_2O NPs

ABTS and DPPH radical scavenging assays were used to evaluate the in vitro antioxidant properties of the SELE-mediated Ag/AgO/Ag_2O NPs. The varying concentrations of the Ag/AgO/Ag_2O NPs and the standard solutions used were 20, 40, 60, 80, and 100 µg/mL. The study employed ascorbic acid as a reference antioxidant. The absorbance was measured to the respective blank solutions using spectrophotometry (Rehana et al. 2017; Jain and Agrawal 2008). The following formula was used to compute the % inhibition:

$$\text{Radical scavenging activity}\,(\%) = \frac{\text{ODcontrol} - \text{ODsample}}{\text{ODcontrol}} \times 100$$

DPPH radical scavenging assay

Serial dilutions (20, 40, 60, 80, and 100 µg/mL) of Ag/AgO/Ag_2O NPs were taken, and 50 µl of 0.659 mM 2,2-diphenyl-1-picrylhydrazyl (DPPH) dissolved in methanol was added, making up to one with distilled water. After that, sample tubes were incubated for 20 min at 25 °C (Jain and Agrawal 2008). A Shimadzu UV 1800 spectrophotometer was employed to record the absorbance at 510 nm.

ABTS radical scavenging assay

Serial dilutions (20, 40, 60, 80, and 100 µg/mL) of Ag/AgO/Ag_2O NPs were taken, and 0.3 ml of ABTS radical cation [ABTS solution: 2, 20-Azino-bis(3-ethylbenzothiazoline-6-sulphonic acid) 2 mM (0.0548 gm in 50 ml)] was prepared in double-distilled water. Potassium persulfate 70 mM was prepared in double-distilled water. After mixing 200 µl of potassium persulphate with 50 ml of ABTS for 2 h, 1.7 ml of phosphate buffer pH 7.4 was mixed. After that, sample tubes were incubated for 20 min at 25 ºC (Jamila et al. 2021). A Shimadzu UV 1800 spectrophotometer was employed to record the absorbance at 734 nm.

DNA Cleavage activity of Ag/AgO/Ag_2O NPs

The DNA cleavage activity of Ag/AgO/Ag_2O NPs was studied using agarose gel electrophoresis. The plasmid DNA (pBR322) was employed as the target DNA for the cleavage activity. Different concentrations of Ag/AgO/Ag_2O NPs and pBR322 DNA molecules were incubated for 30 and 90 min at 37 ºC. After that, loading dye (0.25% bromphenol blue,

50% glycerol) was mixed into the reaction solution. The resulting mixtures were carried out on an electrophoresis gel using 0.8% agarose gel in TAE buffer (50 mM Tris base, 50 mM acetic acid, 2 mM EDTA, pH: 7.8) at 50 V (Gulbagca et al. 2021a). Monitoring was done under UV light after the electrophoresis experiment.

Results and discussion

Structural and morphological study

The phase analysis, crystal structure, and composition of the SELE mediated Ag_xO sample was analyzed through the XRD technique, and the result is evinced in Fig. 2a. It may be observed through this figure that three different phases are present in the sample corresponding to Ag (marked by *), AgO (marked by #), and Ag_2O (marked by ●). This indicates that the current biosynthesis method led to the formation of Ag/AgO/Ag_2O heterostructured NPs. The existence of these phases was identified based on ICDD card no. 04–0783 (Gauri et al. 2016), 84–1108 (Varthini et al. 2018), and 42–0874 for metallic Ag, AgO, and Ag_2O, respectively (Ziashahabi et al. 2019; Yang et al. 2016; Waterhouse et al. 2001). This analysis, therefore, reveals that the three different phases are in the deposited form and not in the doped state since the diffraction peaks of all the phases are visible in the XRD spectrum.

Further, the unassigned peaks belong to $AgNO_3$, which was used as the Ag-precursor in this study (Aziz et al. 2017). This means that the operating temperature was insufficient to eradicate the salt precursor. Nevertheless, based on the intensity of the diffraction peaks, it may be noted that the most dominant phase in this sample is that of AgO. The average crystallite size of the sample was ascertained using Scherrer's equation and found to be 69.4 nm. Based on the XRD result, it is clear that the biosynthesized Ag_xO sample is composed of Ag/AgO/Ag_2O NPs.

It notes that the plant phytochemicals perform two primary functions: (1) bio-reduction of the metal precursor and (2) control over the particle size and shape. Herein, the functionalization of Ag/AgO/Ag_2O NPs by these phytochemicals was confirmed from the FTIR studies. Figure 2b represents the FTIR spectrum of the leaf extract

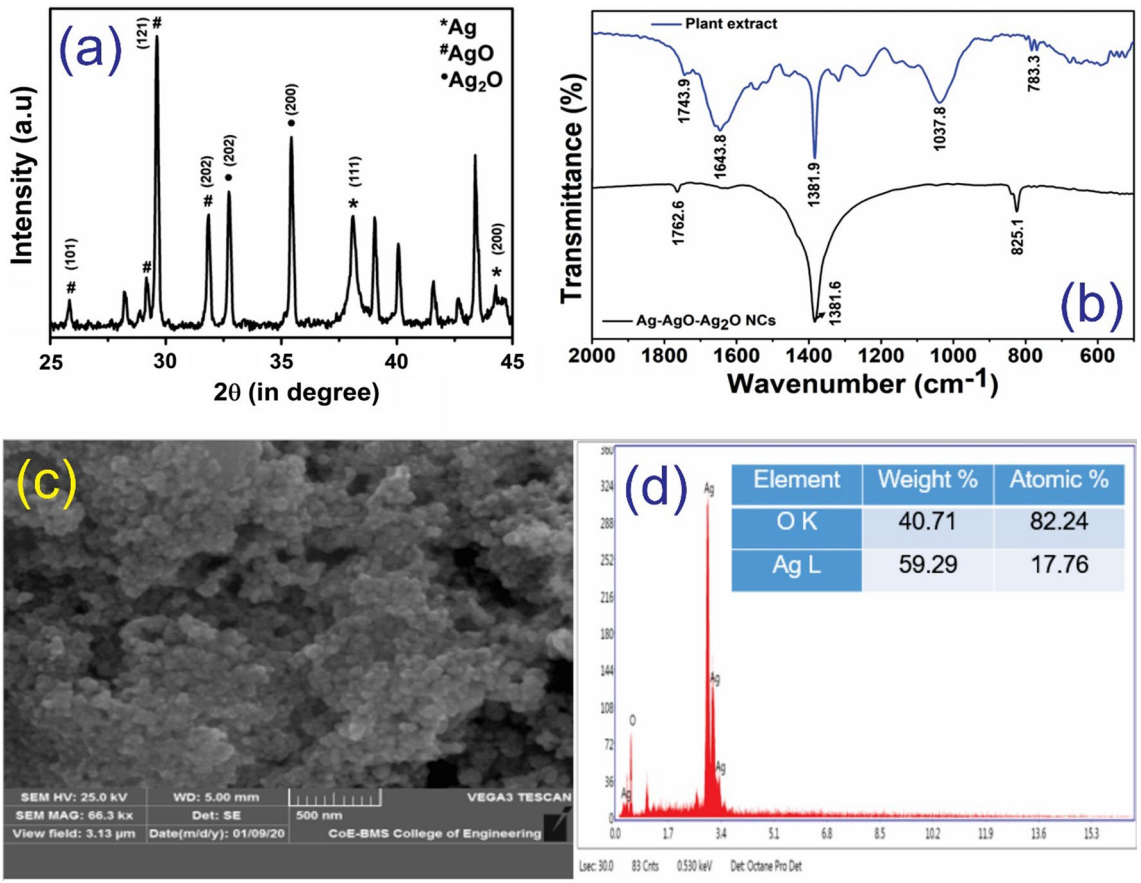

Fig. 2 Characterizations of Ag/AgO/Ag_2O NPs: **a** XRD, **b** FTIR spectra of *Solanum elaeagnifolium* leaf extract (plant extract), and Ag/AgO/Ag_2O NPs, **c** SEM image, and **d** EDX spectra

of *Solanum elaeagnifolium* and Ag/AgO/Ag_2O NPs. On comparing these FTIR spectra, it may be revealed that the bands at 1648.8 cm^{-1} and 1037.8 cm^{-1} of plant extract have wholly lost their intensities after functionalizing the NPs. This means that during the biosynthesis procedure, the functional groups associated with the corresponding phytochemicals were mainly involved in the reducing mechanism of the salt precursor ($AgNO_3$) (Basnet et al. 2018). Contrariwise, the rest of the assigned bands have shifted their positions in the NPs, which may be attributed to their anchoring onto the surface of the NPs. The FTIR bands observed at 1743.9 cm^{-1} in plant extract and 1762.6 cm^{-1} in the NPs correspond to the alkaloid functional group (Masterova and Tomko 1978). The band at 1643.8 cm^{-1} may be ascribed to the C=O stretching vibrations of the amide group majorly because of protein molecules present in the leaf extract (Durak and Depciuch 2020). The highly intense bands at ~ 1381 cm^{-1} may be attributed to the lipid functional group (Velsankar et al. 2020). The band at 1037.8 cm^{-1} represents polysaccharides because of O-substituted glucose residue (Basnet et al. 2019). The band at 783.3 cm^{-1} is due to the C-H out-of-plane bend of phenyl (Basnet et al. 2019). This band has shifted to 825.1 cm^{-1} in the NPs. Thus, based on the relative intensities of the prominent FTIR bands of plant extract and the as-synthesized Ag/AgO/Ag_2O NPs, it may be concluded that protein and glucose metabolites were responsible for functioning as reductants, lipids, and alkaloid functional groups mainly exhibited the capping agent property. This means the latter functional groups have a more vital ability to bind with the Ag ions and prevent their particles from the undesirable agglomeration phenomenon.

A typical SEM analysis was performed to study the morphological characteristic of the as-synthesized Ag/AgO/Ag_2O NPs, as shown in Fig. 2c. In contrast, EDX analysis was employed to detect the elemental composition of this sample, and the results are depicted in Fig. 2d. The SEM image (Fig. 2c) revealed a high density of NPs. Although the particles have mostly agglomerated, it is still possible to clearly distinguish the boundaries between the individual particle grains. From this image, the morphology of the particles was observed to be quasi-spherical in shape. The EDX analysis of Ag/AgO/Ag_2O NPs (Fig. 2d) represents the existence of only Ag and O in the sample with no impurity peaks, indicating the method of biosynthesis employed in this study leads to the formation of impurity-free Ag/AgO/Ag_2O NPs. In addition, the EDX analysis evinced percentage relative elemental composition, such as Ag (17.76%) and O (82.24%), as presented in the inset table of Fig. 2d.

The microstructural analysis and particle size determination of the as-synthesized sample were performed through HRTEM studies, and the results have been shown in Fig. 3. It may be observed from the TEM images in Fig. 3a, b that the particles have formed quasi-spherical microstructure, which is consistent with the morphology obtained through SEM analysis. However, the particles did not exhibit monodispersity, and hence, their average

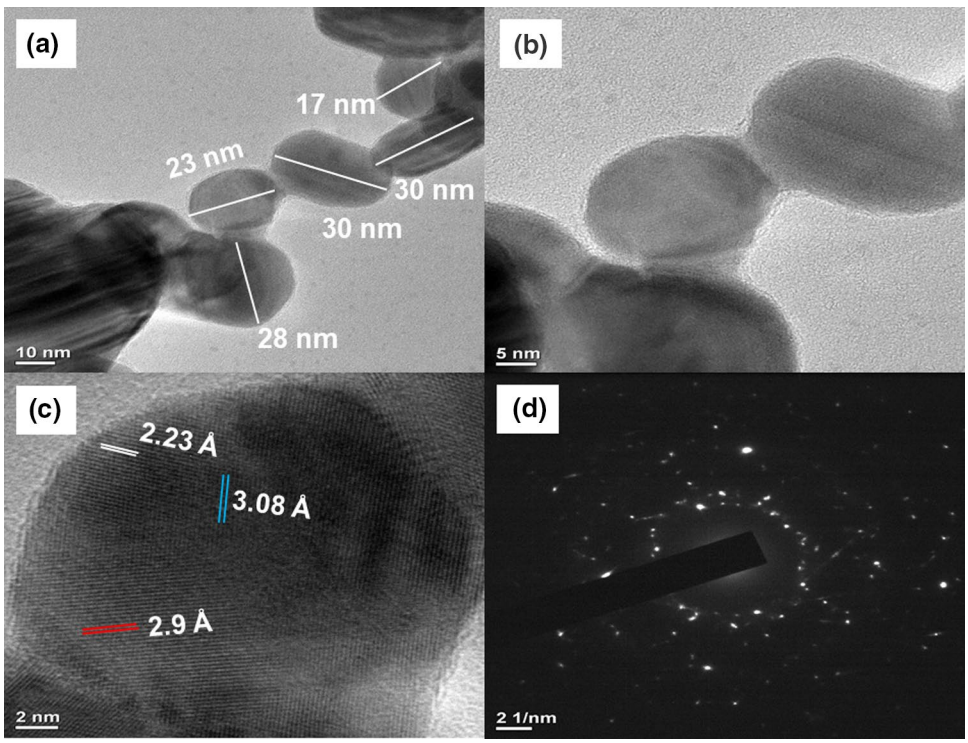

Fig. 3 **a**, **b** TEM image, **c** HRTEM image displaying the lattice fringes, and **d** SAED pattern of Ag/AgO/Ag_2O NPs

diameter was calculated to be in the range of 15–40 nm. Furthermore, from Fig. 3c, which represents the HRTEM image of Ag/AgO/Ag_2O NPs, the appearance of criss-cross patterns is visible, further confirming the existence of different phases in this sample.

The optical absorbance of the as-synthesized sample was analyzed based on the UV–Vis absorbance data, and the corresponding spectra are presented in Fig. 4a. This figure depicts the existence of two major absorbance bands at 295 nm and 455 nm. The band at 295 nm is due to the presence of the AgO component in the sample (Gauri et al. 2016). This means that AgO primarily absorbs in the UV range. The broad absorbance maximum at 455 nm, as shown in Fig. 4b, may be attributed to the absorbance contribution from the Ag and Ag_2O (Ghotekar et al. 2020; Shume et al. 2020) components present in the sample. As a result, the surface plasmon resonance (SPR) effect of Ag NPs (Gauri et al. 2016). Generally, SPR for Ag NPs is observed around 440 nm (Basnet et al. 2019). In this case, a shift in the SPR band may be attributed to the strong interfacial coupling of the Ag NPs with the silver oxide components. Figure 4c represents the Tauc plot fitted using the Tauc equation (Dolgonos et al. 2016) for obtaining the bandgap energy of the as-synthesized sample, which was calculated to be 3.3 eV. Figure 4d corresponds to the PL spectra of the as-synthesized sample. A single emission band centered at 576 nm was observed. This photoluminescence peak corresponds to the bandgap of the as-synthesized NPs as well as its exciting state transition (Lin et al. 2009).

A plausible mechanism for eco-friendly synthesis of Ag/AgO/Ag_2O NPs

The flavonoids/polyphenolic biomolecules have been shown as reducing agents during the plant extract mediated biosynthesis of NPs (Jain and Mehata 2017). The SELE is also a rich source of polyphenolic compounds and flavonoidic groups (Badawy et al. 2013; Elabbar et al. 2014; Balah and AbdelRazek 2020; Hamouda et al. 2015). These polyphenolic compounds as a whole could serve as a reducing agent for Ag^{+1} ion reduction. Figure 5 depicts the schematic representation of a plausible mechanism for Ag ion reduction employing the flavonoids of quercetin of SELE solution. An earlier study using DFT analysis found that the O–H bond dissociation energy of –OH groups of the catechol moiety of flavonoids of quercetin of leaf extract solution is lower than those of other –OH groups in flavonoids (Jain and Mehata 2017). The proposed structure for the Ag-complex development showed that Ag^{+1} could form complexation with quercetin (Aziz et al. 2019) (refer to Fig. 5). When the extract was mixed with the metal salt solution in the first stage, the polyphenolic compounds' –OH groups formed a complex with the Ag^{+1} and reduced it to Ag. Metallic Ag atoms generated in this way react with oxygen to form the

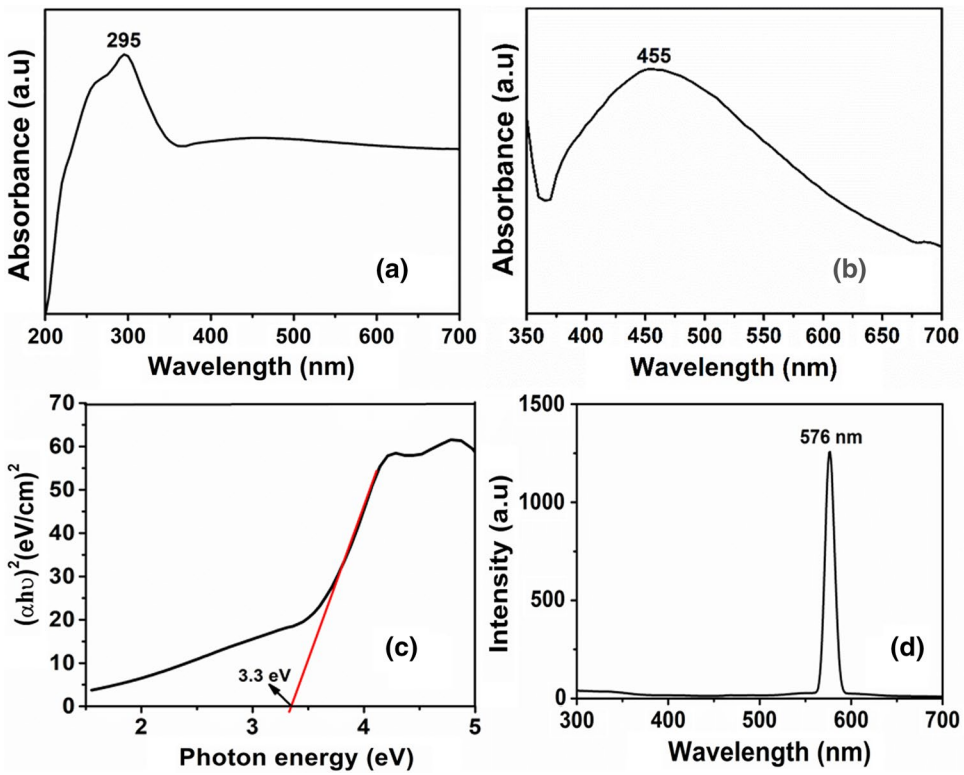

Fig. 4 **a** UV–Vis absorbance spectra of Ag/AgO/Ag_2O NPs, **b** Magnified UV–Vis absorbance spectra ranging from 350 to 700 nm, **c** Tauc-plot for optical band gap energy determination, and **d** PL spectra

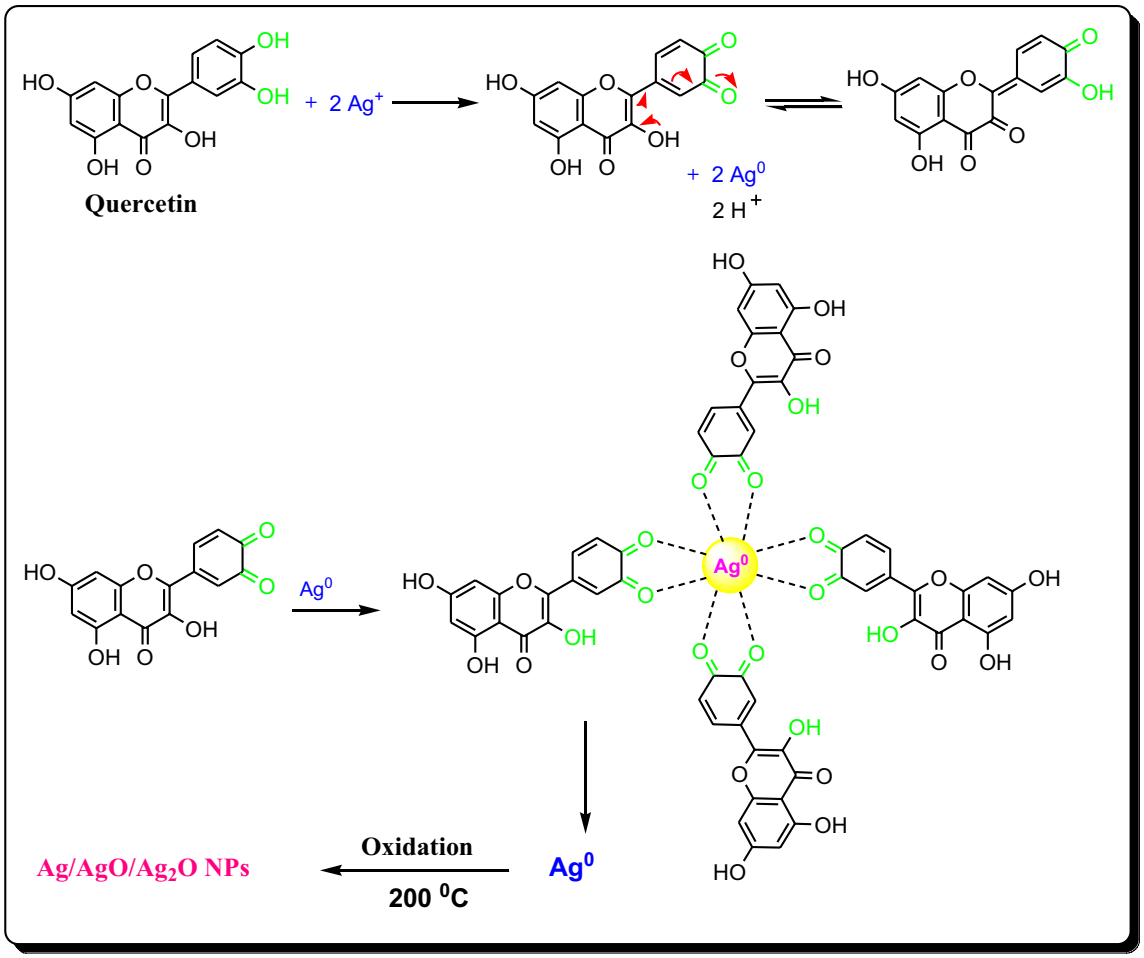

Fig. 5 Plausible mechanism for the synthesis of Ag/AgO/Ag_2O NPs using quercetin as reducing agent

most stable oxides (AgO or Ag_2O). The formation of AgO and Ag_2O is not selective, and hence, we may obtain their mixture. This shows that the current biosynthesis approach led to the formation of Ag/AgO/Ag_2O heterostructured NPs.

Anticancer activity

The anticancer efficacy of SELE mediated Ag/AgO/Ag_2O NPs on human lung cancer cell line (A549) was investigated by MTT assay. For the anticancer study of SELE mediated Ag/AgO/Ag_2O NPs on human lung cancer cell line, diverse concentrations of 10, 20, 40, 60, 80, and 100 µg mL^{-1} were employed, as displayed in Fig. 6. The biogenically fabricated A Ag/AgO/Ag_2O NPs have shown a significant cytotoxicity impact on a human lung cancer cell line, with an IC_{50} value of 67.09 µg mL^{-1}, while Doxorubicin shows an IC_{50} value of 20.66 µg mL^{-1} (Fig. 7). Furthermore, when the concentration of Ag/AgO/Ag_2O NPs was gradually increased to 360 µg mL^{-1} on a human lung cancer cell line, the percentage of cell viability was reduced to 18.28%. The present study results were well supported by diverse research reports (Table 1) on the anticancer effectiveness of the biogenically synthesized AgNPs using the extracts of *Diospyros malabarica, Rosa damascene, Syzygium aromaticum,* and *Ruellia*

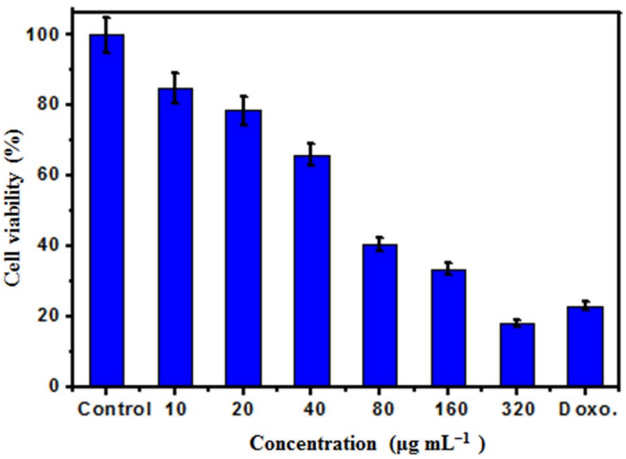

Fig. 6 Anticancer activity of bio-inspired synthesis of Ag/AgO/Ag_2O NPs from SELE

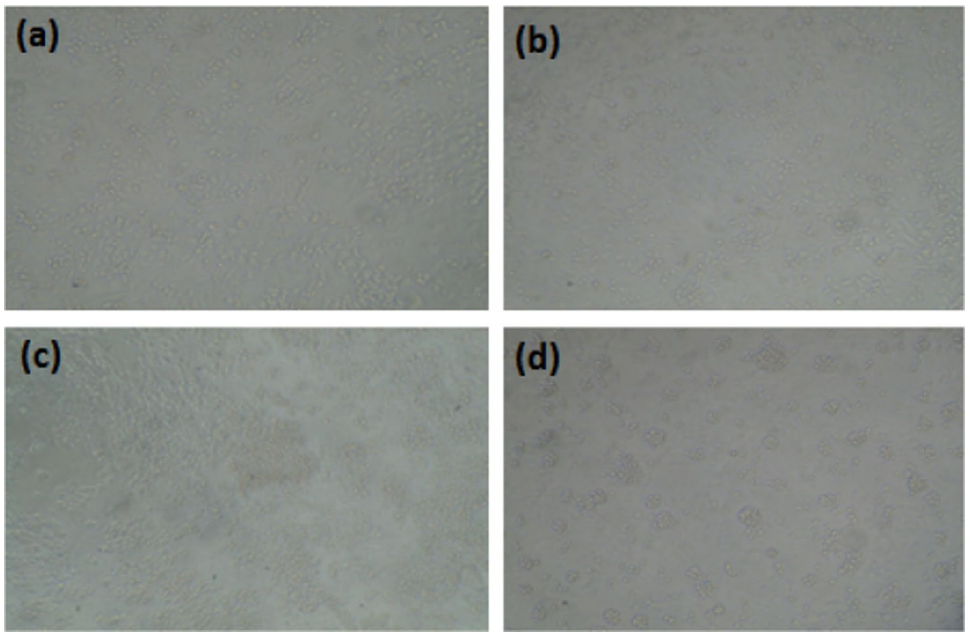

Fig. 7 Anticancer activity of SELE mediated Ag/AgO/Ag_2O NPs, **a** control **b** 10 µg mL^{-1} **c** 360 µg mL^{-1} **d** doxorubicin 100 µg mL^{-1}

Table 1 Comparative study of anticancer activity using NPs for A549-cell lines with previous reports

Name of the plant	Size (nm)	Morphology	IC_{50} (µg/mL)	Reference
Diospyros malabarica	17.4	Spherical	105.8	Bharadwaj et al. 2021)
Rosa damascena	15–27	Spherical	80	Venkatesan et al. 2014)
Syzygium aromaticum	5–40	Spherical	70	Venugopal et al. 2017)
Ruellia tuberosa	55.56	Spherical	68	Seerangaraj et al. 2021)
Solanum elaeagnifolium	69.4	Quasi-spherical	67.09	Present study

tuberosa (Bharadwaj et al. 2021; Venkatesan et al. 2014; Venugopal et al. 2017; Seerangaraj et al. 2021).

Antioxidant activity

The scavenging ability of the Ag/AgO/Ag_2O NPs was evaluated using ABTS and DPPH scavenging assays. The radical scavenging potential of Ag/AgO/Ag_2O NPs was dependent on the concentration, increasing from 20 to 100 g µg mL^{-1} as the concentration of Ag/AgO/Ag_2O NPs (Fig. 8-ABTS and Fig. 9-DPPH). Ag/AgO/Ag_2O NPs also showed considerable ABTS radical scavenging performance with a maximal inhibition of 25.78%. The IC_{50} value of Ag/AgO/Ag_2O NPs against ABTS radicals was 85.12 µg mL^{-1}. Ag/AgO/Ag_2O NPs evinced a maximum scavenging inhibition of 20.86% against DPPH radicals with an IC_{50} value of 89.55 µg mL^{-1}. The antioxidant activity of Ag/AgO/Ag_2O NPs justifies their usefulness in the pharmaceutical and biomedical sectors. These two antioxidant activities were found to increase in a dose-dependent manner. Dose-dependent DPPH antioxidant efficacy by AgNPs synthesized employing *Mangifera indica* seed extract is described by Donga et al. (Donga and Chanda 2021), while Vasiliev et al. (Vorobyova et al. 2020)

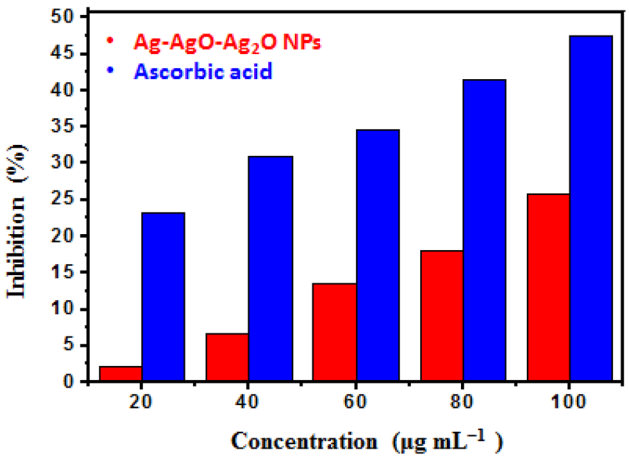

Fig. 8 Antioxidant activities of Ag/AgO/Ag_2O NPs and ascorbic acid using ABTS assay

described by AgNPs synthesized using *black currant pomace* extract. A concentration-dependent increase in ABTS radical scavenging performance is studied by Sathishkumar et al. (Sathishkumar et al. 2019) and Donga et al. (Donga and Chanda 2021).

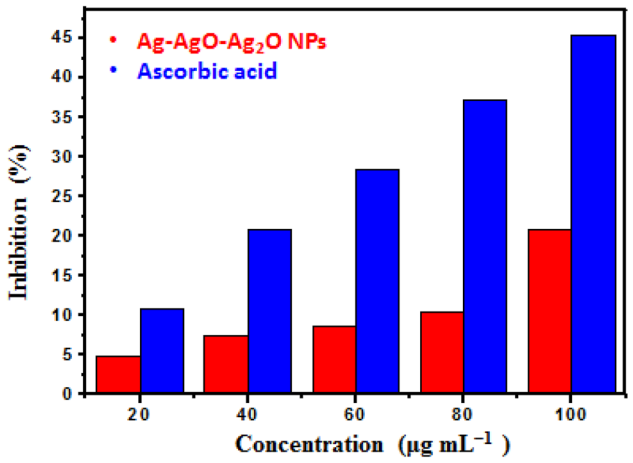

Fig. 9 Antioxidant activities of $Ag/AgO/Ag_2O$ NPs and ascorbic acid using DPPH assay

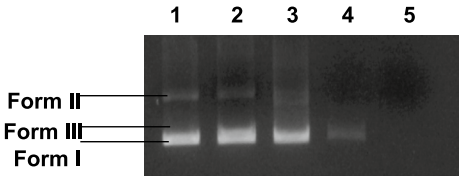

Fig. 10 Lane 1- DNA (control); Lane 2- DNA + H_2O_2 (10 mM); Lane 3- DNA + H_2O_2 + $Ag/AgO/Ag_2O$ NPs (1 µl); Lane 4- DNA + H_2O_2 + $Ag/AgO/Ag_2O$ NPs (2 µl); Lane 5- DNA + H_2O_2 + $Ag/AgO/Ag_2O$ NPs (3 µl)

DNA cleavage activity

The gel electrophoresis was applied to investigate the DNA cleavage activity. Because of its optimal DNA cleavage ability, the biosynthesized $Ag/AgO/Ag_2O$ NPs have a good cleavage performance than the control. $Ag/AgO/Ag_2O$ NPs acted on plasmid DNA molecules, as shown by electrophoresis. The DNA cleavage activity of as-synthesized $Ag/AgO/Ag_2O$ NPs is displayed in Fig. 10. When compared to control DNA, there are changes in the bands of Lanes 2–5, as indicated in Fig. 10. In Lanes 2–4, the plasmid pBR322 was altered from Form I to Form II. Furthermore, the observations revealed that the SELE-mediated $Ag/AgO/Ag_2O$ NPs behaved as chemical nucleases by cleaving DNA Form I into Form III at a concentration of 1 µl for 90 min. This study demonstrated that $Ag/AgO/Ag_2O$ NPs could be employed as an alternative cancer therapy as a DNA target drug. However, few reports showed that green synthesized NPs were used for DNA cleavage study (Gulbagca et al. 2021b; Mousavi-Khattat et al. 2018).

Conclusion

The green chemistry approach was successfully proposed to produce $Ag/AgO/Ag_2O$ NPs composites, and our experiment chose SELE as a natural reducing and/or stabilizing agent. It was revealed that the SELE could be successfully employed for the facile synthesis of $Ag/AgO/Ag_2O$ NPs at room temperature. SELE mediated green synthesizing $Ag/AgO/Ag_2O$ NPs were explored using UVDRS, XRD, FTIR, SEM, HRTEM, EDX, and PL analysis. In the HRTEM analysis of $Ag/AgO/Ag_2O$ NPs, quasi-spherical-shaped particles were obtained. The mean diameter of the $Ag/AgO/Ag_2O$ NPs was 69.4 nm. It was observed that synthesized $Ag/AgO/Ag_2O$ NPs showed sound anticancer effects against A-549 lung cancer cell lines. However, antioxidant and DNA cleavage results have also been effective for $Ag/AgO/Ag_2O$ NPs. The current study has revealed the possibility of executing SELE-mediated $Ag/AgO/Ag_2O$ NPs, which might be exploited as an antioxidant, DNA cleavage, and anticancer agent.

Acknowledgements This work was supported by the Distinguished Scientist Fellowship Program (DSFP) at King Saud University, Riyadh, Saudi Arabia.

References

AlNadhari S, Al-Enazi NM, Alshehrei F, Ameen F (2021) A review on biogenic synthesis of metal nanoparticles using marine algae and its applications. Environ Res 194:110672

Al-Shehri BM, Shkir M, Bawazeer TM, AlFaify S, Hamdy MS (2020) A rapid microwave synthesis of Ag2S nanoparticles and their photocatalytic performance under UV and visible light illumination for water treatment applications. Physica E: Low-dimensional Systems and Nanostructures 121:114060

Aygün A, Özdemir S, Gülcan M, Cellat K, Şen F (2020) Synthesis and characterization of Reishi mushroom-mediated green synthesis of silver nanoparticles for the biochemical applications. J Pharm Biomed Anal 178:112970

Ayodhya D, Veerabhadram G (2016) Green synthesis, characterization, photocatalytic, fluorescence and antimicrobial activities of Cochlospermum gossypium capped Ag2S nanoparticles. J Photochem Photobiol, B 157:57–69

Aziz SB, Abdulwahid RT, Rasheed MA, Abdullah OG, Ahmed HM (2017) Polymer blending as a novel approach for tuning the SPR peaks of silver nanoparticles. Polymers 9:486

Aziz SB, Hussein G, Brza M, Mohammed SJ, Abdulwahid RT, Raza Saeed S, Hassanzadeh A (2019) Fabrication of interconnected plasmonic spherical silver nanoparticles with enhanced localized surface plasmon resonance (LSPR) peaks using quince leaf extract solution. Nanomaterials 9:1557

Babu PJ, Doble M, Raichur AM (2018) Silver oxide nanoparticles embedded silk fibroin spuns: microwave mediated preparation, characterization and their synergistic wound healing and antibacterial activity. J Colloid Interface Sci 513:62–71

Badawy A, Zayed R, Ahmed S, Hassanean H (2013) Phytochemical and pharmacological studies of Solanum elaeagnifolium growing in Egypt. J Nat Prod 6:156–167

Balah MA, AbdelRazek GM (2020) Pesticidal activity of Solanum elaeagnifolium Cav Leaves against Nematodes and Perennial Weeds. Acta Ecologica Sinica 40:373–379

Bandeira M, Giovanela M, Roesch-Ely M, Devine DM, da Silva Crespo J (2020) Green synthesis of zinc oxide nanoparticles: a review of the synthesis methodology and mechanism of formation. Sustain Chem Pharm 15:100223

Basnet P, Chanu TI, Samanta D, Chatterjee S (2018) A review on bio-synthesized zinc oxide nanoparticles using plant extracts as reductants and stabilizing agents. J Photochem Photobiol, B 183:201–221

Basnet P, Samanta D, Chanu TI, Mukherjee J, Chatterjee S (2019) Teaphytochemicals functionalized Ag modified ZnO nanocomposites for visible light driven photocatalytic removal of organic water pollutants. Materials Research Express 6:085095

Bharadwaj KK, Rabha B, Pati S, Choudhury BK, Sarkar T, Gogoi SK, Kakati N, Baishya D, Kari ZA, Edinur HA (2021) Green synthesis of silver nanoparticles using Diospyros malabarica fruit extract and assessments of their antimicrobial, anticancer and catalytic reduction of 4-nitrophenol (4-NP). Nanomaterials 11:1999

Bhosale MA, Bhanage BM (2015) Silver nanoparticles: synthesis, characterization and their application as a sustainable catalyst for organic transformations. Curr Org Chem 19:708–727

Cuong HN, Pansambal S, Ghotekar S, Oza R, Hai NTT, Viet NM, Nguyen V-H (2021) New frontiers in the plant extract mediated biosynthesis of copper oxide (CuO) nanoparticles and their potential applications: a review. Environ Res 203:111858

Dabhane H, Ghotekar SK, Tambade PJ, Pansambal S, Ananda Murthy H, Oza R, Medhane V (2021) Cow urine mediated green synthesis of nanomaterial and their applications: a state-of-the-art review. J Water And Environ Nanotechnol 6:81–91

Devadas B, Periasamy AP, Bouzek K (2021) A review on poly (amidoamine) dendrimer encapsulated nanoparticles synthesis and usage in energy conversion and storage applications. Coord Chem Rev 444:214062

Dolgonos A, Mason TO, Poeppelmeier KR (2016) Direct optical band gap measurement in polycrystalline semiconductors: A critical look at the Tauc method. J Solid State Chem 240:43–48

Donga S, Chanda S (2021) Facile green synthesis of silver nanoparticles using Mangifera indica seed aqueous extract and its antimicrobial, antioxidant and cytotoxic potential (3-in-1 system). Artif Cells, Nanomed, Biotechnol 49:292–302

Durak T, Depciuch J (2020) Effect of plant sample preparation and measuring methods on ATR-FTIR spectra results. Environ Exp Bot 169:103915

Durán N, Nakazato G, Seabra AB (2016) Antimicrobial activity of biogenic silver nanoparticles, and silver chloride nanoparticles: an overview and comments. Appl Microbiol Biotechnol 100:6555–6570

Elabbar FA, Bozkeha NM, El-Tuonsia AT (2014) Extraction, separation and identification of compounds from leaves of Solanum elaeagnifolium Cav (Solanaceae). Int Curr Pharm J 3:234–239

Gauri B, Vidya K, Sharada D, Shobha W (2016) Synthesis and characterization of Ag/AgO nanoparticles as alcohol sensor. Res J Chem Environ 20:1–5

Gawande MB, Goswami A, Felpin F-X, Asefa T, Huang X, Silva R, Zou X, Zboril R, Varma RS (2016) Cu and Cu-based nanoparticles: synthesis and applications in catalysis. Chem Rev 116:3722–3811

Ghotekar S (2019) A review on plant extract mediated biogenic synthesis of CdO nanoparticles and their recent applications. Asian J Green Chem 3:187–200

Ghotekar S, Pansambal S, Pawar SP, Pagar T, Oza R, Bangale S (2019) Biological activities of biogenically synthesized fluorescent silver nanoparticles using Acanthospermum hispidum leaves extract. SN Applied Sciences 1:1–12

Ghotekar S, Dabhane H, Pansambal S, Oza R, Tambade P, Medhane V (2020) A review on biomimetic synthesis of Ag2O nanoparticles using plant extract, characterization and its recent applications. Adv J Chem-Sect B 2:102–111

Ghotekar S, Pagar K, Pansambal S, Murthy HA and Oza R (2021) Biosynthesis of silver sulfide nanoparticle and its applications. In: Handbook of greener synthesis of nanomaterials and compounds, Elsevier, pp 191–200

Göl F, Aygün A, Seyrankaya A, Gür T, Yenikaya C, Şen F (2020) Green synthesis and characterization of Camellia sinensis mediated silver nanoparticles for antibacterial ceramic applications. Materials Chemistry and Physics 250:123037

Gonzalez R, Tarloff J (2001) Evaluation of hepatic subcellular fractions for Alamar blue and MTT reductase activity. Toxicol in Vitro 15:257–259

Gulbagca F, Aygün A, Gülcan M, Ozdemir S, Gonca S, Şen F (2021a) Green synthesis of palladium nanoparticles: Preparation, characterization, and investigation of antioxidant, antimicrobial, anticancer, and DNA cleavage activities. Applied Organometallic Chemistry 35:e6272

Gulbagca F, Aygün A, Gülcan M, Ozdemir S, Gonca S, Şen F (2021) Green synthesis of palladium nanoparticles: preparation, characterization, and investigation of antioxidant, antimicrobial, anticancer, and DNA cleavage activities. Appl Organomet Chem 35:e6272

Gur T, Meydan I, Seckin H, Bekmezci M, Sen F (2022) Green synthesis, characterization and bioactivity of biogenic zinc oxide nanoparticles. Environ Res 204:111897

Hamouda AB, Zarrad K, Laarif A, Chaieb I (2015) Insecticidal effect of Solanum elaeagnifolium extracts under laboratory conditions. J Entomol Zool Stud 3:187–190

Hosseinpour-Mashkani SM, Ramezani M (2014) Silver and silver oxide nanoparticles: synthesis and characterization by thermal decomposition. Mater Lett 130:259–262

Ibrahim S, Ahmad Z, Manzoor MZ, Mujahid M, Faheem Z, Adnan A (2021) Optimization for biogenic microbial synthesis of silver nanoparticles through response surface methodology, characterization, their antimicrobial, antioxidant, and catalytic potential. Sci Rep 11:1–18

Jain P, Agrawal R (2008) Antioxidant and free radical scavenging properties of developed mono-and polyherbal formulations. Asian J Exp Sci 22:213–220

Jain S, Mehata MS (2017) Medicinal plant leaf extract and pure flavonoid mediated green synthesis of silver nanoparticles and their enhanced antibacterial property. Sci Rep 7:1–13

Jamila N, Khan N, Bibi N, Waqas M, Khan SN, Atlas A, Amin F, Khan F, Saba M (2021) Hg (II) sensing, catalytic, antioxidant, antimicrobial, and anticancer potential of Garcinia mangostana and α-mangostin mediated silver nanoparticles. Chemosphere 272:129794

Lin W (2015) Introduction: nanoparticles in medicine. Chem Rev 115:10407–10409

Lin T-H, Chen T-T, Cheng C-L, Lin H-Y, Chen Y-F (2009) Selectively enhanced band gap emission in ZnO/Ag 2 O nanocomposites. Opt Express 17:4342–4347

Marimuthu S, Antonisamy AJ, Malayandi S, Rajendran K, Tsai P-C, Pugazhendhi A, Ponnusamy VK (2020) Silver nanoparticles in dye effluent treatment: A review on synthesis, treatment methods, mechanisms, photocatalytic degradation, toxic effects and mitigation of toxicity. J Photochem Photobiol B: Biol 205:111823

Masterova I, Tomko J (1978) Isolation and identification of alkaloids from Frítillaria imperíalis L. var. rubra maxima. Chem zvesti 32:116–119

Matussin S, Harunsani MH, Tan AL, Khan MM (2020) Plant-extract-mediated SnO2 nanoparticles: synthesis and applications. ACS Sustain Chem & Eng 8:3040–3054

Mousavi-Khattat M, Keyhanfar M, Razmjou A (2018) A comparative study of stability, antioxidant DNA cleavage and antibacterial activities of green and chemically synthesized silver nanoparticles. Artif Cells, Nanomed, Biotechnol 46:S1022–S1031

Nasrollahzadeh M, Sajjadi M, Dadashi J, Ghafuri H (2020) Pd-based nanoparticles: plant-assisted biosynthesis, characterization, mechanism, stability, catalytic and antimicrobial activities. Adv Colloid Interface Sci 276:102103

Nikam A, Pagar T, Ghotekar S, Pagar K, Pansambal S (2019) A review on plant extract mediated green synthesis of zirconia nanoparticles and their miscellaneous applications. J Chem Rev 1:154–163

Partila AM (2019) Bioproduction of silver nanoparticles and its potential applications in agriculture. In: Nanotechnology for agriculture, Springer, Singapore, pp 19–36

Patra JK, Baek K-H (2016) Green synthesis of silver chloride nanoparticles using Prunus persica L. outer peel extract and investigation of antibacterial, anticandidal, antioxidant potential. Green Chem Lett Rev 9:132–142

Rashmi B, Harlapur SF, Avinash B, Ravikumar C, Nagaswarupa H, Kumar MA, Gurushantha K, Santosh M (2020) Facile green synthesis of silver oxide nanoparticles and their electrochemical, photocatalytic and biological studies. Inorganic Chemistry Communications 111:107580

Rehana D, Mahendiran D, Kumar RS, Rahiman AK (2017) Evaluation of antioxidant and anticancer activity of copper oxide nanoparticles synthesized using medicinally important plant extracts. Biomed Pharmacother 89:1067–1077

Sangeetha TV, Mohanapriya S (2021) Synthesis, characterization and biological evaluation of heterocyclic triazole derived Schiff base ligands comprising Mn (II) complexes: Implications of their DNA/protein binding docking and anticancer activity studies. Indian Journal of Chemistry-Section A (IJCA). 60(6):797–805

Santhosh A, Theertha V, Prakash P, Chandran SS (2021) From waste to a value added product: green synthesis of silver nanoparticles from onion peels together with its diverse applications. Mater Today: Proc 46:4460–4463

Sathishkumar R, Sundaramanickam A, Srinath R, Ramesh T, Saranya K, Meena M, Surya P (2019) Green synthesis of silver nanoparticles by bloom forming marine microalgae Trichodesmium erythraeum and its applications in antioxidant, drug-resistant bacteria, and cytotoxicity activity. J Saudi Chem Soc 23:1180–1191

Seerangaraj V, Sathiyavimal S, Shankar SN, Nandagopal JGT, Balashanmugam P, Al-Misned FA, Shanmugavel M, Senthilkumar P, Pugazhendhi A (2021) Cytotoxic effects of silver nanoparticles on Ruellia tuberosa: Photocatalytic degradation properties against crystal violet and coomassie brilliant blue. J Environ Chem Eng 9:105088e

Shahjahan M, Rahman H, Hossain MS, Khatun MA, Islam A, Begum MHA (2017) Synthesis and characterization of silver nanoparticles by sol-gel technique. Nanosci Nanometrol 3:34–39

Sharma RK, Yadav S, Dutta S, Kale HB, Warkad IR, Zbořil R, Varma RS and Gawande MB (2021) Silver nanomaterials: synthesis and (electro/photo) catalytic applications. Chem Soc Rev

Shume WM, Murthy HC and Zereffa EA (2020) A review on synthesis and characterization of Ag2O nanoparticles for photocatalytic applications. J Chem, 2020

Singh SP, Bhargava C, Dubey V, Mishra A, Singh Y (2017) Silver nanoparticles: biomedical applications, toxicity, and safety issues. Int J Res Pharm Pharm Sci 4:01–10

Soni V, Raizada P, Singh P, Cuong HN, Rangabhashiyam S, Saini A, Saini RV, Van Le Q, Nadda AK, Le T-T (2021) Sustainable and green trends in using plant extracts for the synthesis of biogenic metal nanoparticles toward environmental and pharmaceutical advances: a review. Environ Res 202:111622

Tagad CK, Dugasani SR, Aiyer R, Park S, Kulkarni A, Sabharwal S (2013) Green synthesis of silver nanoparticles and their application for the development of optical fiber based hydrogen peroxide sensor. Sens Actuators, B Chem 183:144–149

Thanh NT, Maclean N, Mahiddine S (2014) Mechanisms of nucleation and growth of nanoparticles in solution. Chem Rev 114:7610–7630

Varthini T, Carmel Vijila G, Jothi M (2018) Effect of medicinal leaf extract in silver nitrate-size reduction to nanoscale. J Emerg Tech Innov Res 5:664–666

Velsankar K, Sudhahar S, Parvathy G, Kaliammal R (2020) Effect of cytotoxicity and aAntibacterial activity of biosynthesis of ZnO hexagonal shaped nanoparticles by Echinochloa frumentacea grains extract as a reducing agent. Mater Chem Phys 239:121976

Venkatesan B, Subramanian V, Tumala A, Vellaichamy E (2014) Rapid synthesis of biocompatible silver nanoparticles using aqueous extract of Rosa damascena petals and evaluation of their anticancer activity. Asian Pac J Trop Med 7:S294–S300

Venugopal K, Rather H, Rajagopal K, Shanthi M, Sheriff K, Illiyas M, Rather R, Manikandan E, Uvarajan S, Bhaskar M (2017) Synthesis of silver nanoparticles (Ag NPs) for anticancer activities (MCF 7 breast and A549 lung cell lines) of the crude extract of Syzygium aromaticum. J Photochem Photobiol, B 167:282–289

Vorobyova V, Vasyliev G, Skiba M (2020) Eco-friendly "green" synthesis of silver nanoparticles with the black currant pomace extract and its antibacterial, electrochemical, and antioxidant activity, Applied. Nanoscience 10:4523–4534

Waterhouse GI, Bowmaker GA, Metson JB (2001) The thermal decomposition of silver (I, III) oxide: A combined XRD, FT-IR and Raman spectroscopic study. Phys Chem Chem Phys 3:3838–3845

Yang J, Pan J (2012) Hydrothermal synthesis of silver nanoparticles by sodium alginate and their applications in surface-enhanced Raman scattering and catalysis. Acta Mater 60:4753–4758

Yang H, Ren Y-Y, Wang T, Wang C (2016) Preparation and antibacterial activities of Ag/Ag+/Ag3+ nanoparticle composites made by pomegranate (Punica granatum) rind extract. Results Phys 6:299–304

Yew YP, Shameli K, Miyake M, Khairudin NBBA, Mohamad SEB, Naiki T, Lee KX (2020) Green biosynthesis of superparamagnetic magnetite Fe3O4 nanoparticles and biomedical applications in targeted anticancer drug delivery system: a review. Arab J Chem 13:2287–2308

Ziashahabi A, Prato M, Dang Z, Poursalehi R, Naseri N (2019) The effect of silver oxidation on the photocatalytic activity of Ag/ZnO hybrid plasmonic/metal-oxide nanostructures under visible light and in the dark. Sci Rep 9:1–12

Authors and Affiliations

Mukul Barwant[1] · Yogrsh Ugale[1] · Suresh Ghotekar[2] · Parita Basnet[3] · Van-Huy Nguyen[4] · Shreyas Pansambal[5] · H. C. Ananda Murthy[6] · Mika Sillanpaa[7,8] · Muhammad Bilal[9] · Rajeshwari Oza[10] · Vanita Karande[11]

1 Department of Chemistry, Sanjivani Arts, Commerce and Science College, Savitribai Phule Pune University, Kopargaon, Maharashtra 423603, India

2 Department of Chemistry, Smt. Devkiba Mohansinhji Chauhan College of Commerce and Science, University of Mumbai, Silvassa, Dadra and Nagar Haveli (UT) 396230, India

3 Centre for Materials Science and Nanotechnology, Sikkim Manipal Institute of Technology, Sikkim Manipal University, Gangtok, Sikkim, India

4 Faculty of Allied Health Sciences, Chettinad Academy of Research and Education (CARE), Kelambakkam, Chennai, Tamilnadu 603 103, India

5 Department of Chemistry, Shri Saibaba College Shirdi, Savitribai Phule Pune University, Shirdi, Maharashtra 423109, India

6 Department of Applied Chemistry, School of Applied Natural Sciences, Adama Science and Technology University, P.O. Box: 1888, Adama, Ethiopia

7 Department of Chemical Engineering, School of Mining, Metallurgy and Chemical Engineering, University of Johannesburg, P. O. Box 17011, Doornfontein 2028, South Africa

8 Chemistry Department, College of Science, King Saud University, Riyadh 11451, Saudi Arabia

9 School of Life Science and Food Engineering, Huaiyin Institute of Technology, Huaian 223003, China

10 Department of Chemistry, D.J.M. Commerce and B.N.S. Science College, Savitribai Phule Pune University, S.N. Arts, Sangamner, Maharashtra 422605, India

11 Department of Botany, Yashavantrao Chavan Institute of Science, Satara, Maharashtra 415001, India